Presynaptic glutamatergic transmission and feedback system of oxytocinergic neurons in the hypothalamus of a rat model of adjuvant arthritis

Teruaki Fujitani[1],*, Takanori Matsuura[1,2],*, Makoto Kawasaki[1] (ID),
Hitoshi Suzuki[1], Haruki Nishimura[1], Kazuhiko Baba[1],
Yoshiaki Yamanaka[1], Hideo Ohnishi[1], Yoichi Ueta[2], and
Akinori Sakai[1]

Abstract

The neurohypophysial hormone oxytocin (OXT) is synthesized in the hypothalamic paraventricular and supraoptic nuclei. Recently, some studies have considered OXT to be important in sensory modulation and that the OXT protein is upregulated by acute and chronic nociception. However, the mechanism by which OXT is upregulated in neurons is unknown. In this study, we examined the resting membrane potentials and excitatory postsynaptic currents in OXT-ergic neurons in the paraventricular nucleus in adjuvant arthritis rat model, a model of chronic inflammation, using whole-cell patch-clamping. Transgenic rats expressing OXT and monomeric red fluorescent protein 1 (mRFP1) fusion protein to visualize the OXT-ergic neurons were used, and the OXT-mRFP1 transgenic rat model of adjuvant arthritis was developed by injection of heat-killed *Mycobacterium butyricum*. Furthermore, the feedback system of synthesized OXT was also examined using the OXT receptor antagonist L-368,899. We found that the resting membrane potentials and frequency of miniature excitatory postsynaptic currents and spontaneous excitatory postsynaptic currents in OXT-monomeric red fluorescent protein 1 neurons in the paraventricular nucleus were significantly increased in adjuvant arthritis rats. Furthermore, L-368,899 dose-dependently increased the frequency of miniature excitatory postsynaptic currents and spontaneous excitatory postsynaptic currents in OXT-ergic neurons. Following bath application of the GABA$_A$ receptor antagonist picrotoxin and the cannabinoid receptor 1 antagonist AM 251, L-368,899 still increased the frequency of miniature excitatory postsynaptic currents. However, following bath application of the nitric oxide synthase inhibitor Nω-Nitro-L-arginine methyl ester hydrochloride, L-368,899 did not alter the miniature excitatory postsynaptic current frequency. Thus, it is suggested that OXT-ergic neuron activity is upregulated via an increase in glutamate release, and that the upregulated OXT neurons have a feedback system with released endogenous OXT. It is possible that nitric oxide, but not GABA, may contribute to the feedback system of OXT neurons in chronic inflammation.

Introduction

Oxytocin (OXT), a neurohypophysial hormone, is synthesized in the hypothalamic paraventricular nucleus (PVN) and supraoptic nucleus (SON) and enters the systemic circulation from the posterior pituitary. The functions of OXT are classically considered to be the contraction of the uterus and the milk reflex during

[1]Department of Orthopaedic Surgery, School of Medicine, University of Occupational and Environmental Health, Kitakyushu, Japan
[2]Department of Physiology, School of Medicine, University of Occupational and Environmental Health, Kitakyushu, Japan

*The first two authors contributed equally to this work.

Corresponding Author:
Makoto Kawasaki, Department of Orthopaedic Surgery, School of Medicine, University of Occupational and Environmental Health, 1–1 Iseigaoka, Yahatanishi-ku, Kitakyushu 807-8555, Japan.
Email: k-makoto@med.uoeh-u.ac.jp

lactation. Recently, it has been shown that OXT is also involved in maternal bonding, sexual behavior, and social affiliation.[1,2] Furthermore, some studies have suggested that OXT is important in sensory modulation.[3] For example, OXT attenuates inflammation and myeloperoxidase activity induced by the subcutaneous injection of carrageenan[4]; subarachnoid administration of OXT lowers the threshold of pain,[5] and transient OXT administration abolishes hypersensitivity in the nerve injury rat model.[6] In addition, it is known that the activity of OXT-ergic neurons is upregulated by various stresses, such as conditioned fear (environmental stimuli previously paired with foot shocks), unconditioned fear (intermittently applied foot shocks), noxious stimuli,[7–10] and morphine withdrawal.[11] A previous study reported that OXT was upregulated in the PVN, SON, posterior pituitary, and the dorsal horn of the spinal cord in rats with adjuvant arthritis (AA), which is a well-known chronic pain model.[12] However, the mechanism by which OXT-ergic neuron activity is upregulated is not known. *In vivo* electrophysiological studies of rats and mice have demonstrated that peripheral chronic nociceptive stimulation and/or injury models produce evoked action potentials (APs) or excitatory presynaptic potentials (EPSPs) in the central nervous system.[13] However, previous studies have not examined whether the mechanism involves OXT-ergic neurons.

The hypothalamic PVN generates a homeostatic response.[14] It has been shown that neuroendocrine-autonomic integration is a homeostatic response in the PVN,[15] and that the activity-dependent dendritic release of OXT from the PVN acts diffusely to increase the activity of presympathetic neurons.[14] The dendrites release OXT, which then functions as a paracrine or autocrine signal at the site of release.[16] However, the mechanism of communication between OXT-ergic neurons is not well understood.

In this study, we investigated excitatory postsynaptic currents (EPSCs) in OXT-ergic neurons in the PVN in an AA rat model using whole-cell patch-clamping. A previous study demonstrated that *OXT* mRNA could not be distinguished from *vasopressin* mRNA in magnocellular neuroendocrine cells in the hypothalamus using the polymerase chain reaction (PCR) method.[17] Thus, in these experiments, we used transgenic rats that expressed the OXT-monomeric red fluorescent protein 1 (mRFP1) fusion protein to enable the visualization of OXT-ergic neurons.[18] The OXT-mRFP1 transgenic rat is useful for studying the electrophysiology of the hypothalamo-neurohypophysial system because OXT neurons can be detected easily using fluorescence microscopy. We hypothesize that the OXT synthesized in AA rats affects the feedback system, including the EPSPs between OXT-ergic neurons. We investigated the detailed feedback system of synthesized OXT by using an OXT antagonist. In addition, we examined the contribution of retrograde synaptic transmitters in the feedback system of OXT-ergic neurons.

Materials and methods

Animals

We used OXT-mRFP1 transgenic rats (Wistar, male, aged six to eight weeks and weighing 200–300 g) that were bred and maintained as described previously.[18] All rats received food and water ad libitum and were maintained on a 12:12 h light/dark cycle (lights on at 07.00 h) at 22°C to 25°C, with three rats housed per plastic cage. PCR for genomic DNA was performed for all rats to confirm the presence of the *OXT-mRFP1* gene.

AA model

We intracutaneously (i.c.) injected heat-killed *Mycobacterium butyricum* (1 mg/rat) in paraffin liquid into OXT-mRFP1 transgenic rats via their tail root.[12] In the same manner, we injected 100 µl of paraffin liquid i.c. via the tail root of control rats. The arthritis index (AI) was scored before decapitation. The severity of arthritis in the paw of each rat was graded from 0 to 4. Grade 0 indicates no swelling. Grade 1 indicates mild swelling or erythema on only one toe. Grade 2 indicates swelling of one or more toes. Grade 3 indicates swelling of the ankle. Grade 4 indicates severe swelling of the toes and the ankle.

Slice preparations

The rats were killed by decapitation on day 15 postinjection (vehicle or heat-killed *M. butyricum* in paraffin liquid). After removing each brain from the skull, we confirmed that there was no significant hemorrhage or gross contusion. The brains were placed in cold oxygenated (5% CO_2 and 95% O_2) cutting solution containing 252 mM sucrose, 6 mM $MgSO_4$, 2.5 mM KCl, 0.5 mM $CaCl_2$, 1.2 mM NaH_2PO_4, 25 mM $NaHCO_3$, and 10 mM glucose. We cut the brain including the hypothalamus and glued it using instant adhesive onto the stage of a vibratome-type slicer (DSK Linearslicer PRO7, Kyoto, Japan). As described previously, coronal slices (300 µm thick) containing the PVN were cut after carefully removing the meninges.[19] The slices were preincubated in artificial cerebrospinal fluid (ACSF) containing 124 mM NaCl, 2 mM $CaCl_2$, 2.5 mM KCl, 2 mM $MgSO_4$, 1 mM NaH_2PO_4, 10 mM glucose, and 25 mM $NaHCO_3$ at room temperature for at least 1 h, and then the slices were transferred to the recording chamber.[20]

In vitro *patch-clamp recordings*

We placed the brain slices onto a glass-bottomed chamber and fixed the brain slice using a grid of parallel nylon

threads supported by the weight of the C-shaped stainless steel. A low-pressure aspiration system kept the solution level constant. To identify the mRFP1-positive neurons, an upright microscope (BX-50, Olympus) and infrared differential interference contrast (DIC) optics with an mRFP1 filter (Olympus) were used. We acquired signals filtered at 3 kHz with a patch-clamp amplifier (Axopatch 200B; Axon Instruments, Sunnyvale, CA, USA) and digitized it at 1 kHz with an analog to digital converter (Digidata 1440 A; Axon Instruments). Spontaneous EPSCs (sEPSCs) were recorded from OXT-mRFP1 neurons in the magnocellular PVN (mPVN) of the hypothalamus. The neurons were voltage-clamped at -60 mV for sEPSCs and miniature EPSCs (mEPSC) or 0 mV for miniature inhibitory postsynaptic currents (mIPSCs). We filled the recording pipettes (3–6 MΩ) with a solution containing 145 mM K-gluconate, 1 mM $MgCl_2$, 5 mM NaCl, 10 mM HEPES, 2 mM Mg-ATP, 0.2 mM EGTA, and 0.1 mM Na_3-GTP (adjusted to pH 7.2 with KOH). The membrane potential was held at -60 mV, except during these experiments. We waited for 5 min after the formation of whole-cell recordings to allow the resting membrane potentials (RMPs) to stabilize, unless stated otherwise. Using the property that glutamic voluntary quantum release is insensitive to Na^+ channel interception, we used tetrodotoxin (1 μM) to separate mEPSCs from other currents. mIPSCs were recorded with bath presence of cyanquixaline (20 μM), (2 R)-amino-5-phosphonopentanoate (50 μM), and holding voltage 0 mV. The patch electrode internal solution (112 mM Cs-gluconate, 5 mM TEA-Cl, 3.7 mM NaCl, 10 mM HEPES, 2 mM Mg-ATP, 0.2 mM EGTA, 0.3 mM Na_3-GTP, and 5 mM QX-314, pH adjusted to 7.2 using CsOH) was used for recording mIPSCs.

Drug application

GABA$_A$ receptor antagonist (picrotoxin), OXT, and Nω-Nitro-L-arginine methyl ester hydrochloride (L-NAME) were obtained from Sigma Aldrich (St. Louis, MO, USA). The OXT receptor antagonist (L-368,899) and cannabinoid receptor 1 antagonist (AM 251) were obtained from Tocris Cookson (Bristol, UK). Immediately before use, all drugs used were diluted from stock solutions to the final desired concentration in ACSF.

Data analysis

The data were collected and analyzed with Clampex 10.7 and Clampfit 10.7 (Molecular Devices, San Jose, CA, USA). An unpaired student's *t* test, paired *t* test, or one-way analysis of variance (ANOVA) was used for comparisons between the two groups. The data are shown as means ± standard error of the mean. In all cases, differences with $p < 0.05$ were deemed to be statistically significant.

Results

In vitro *whole-cell patch-clamp recording of the hypothalamic mPVN in the OXT-mRFP1 transgenic rat*

Whole-cell patch-clamp recordings of OXT-mRFP1 neurons were performed in the mPVN of OXT-mRFP1 transgenic rats (Figure 1(A), left). The mRFP1 fluorescence was observed in the PVN by fluorescence microscopy (Figure 1(A), right). The OXT-mRFP1 neurons were distinguishable from other neurons by DIC fluorescence in the PVN (Figure 1(B), a to f).

Electrophysiological response of OXT-mRFP1 neurons in the PVN using whole-cell patch-clamp recordings . We confirmed AI to evaluate the degree of inflammation on the day of the experiment. AI of AA rats was significantly higher than in the control rats (control group: 0, $n = 6$ rats; AA group: 11.83 ± 1.14, $n = 6$ rats; one-way ANOVA, $F_{1,10} = 108.17$, $p = 0.0000011$, Figure 2(a)). We examined the RMPs using whole-cell patch-clamp recordings of neurons in the PVN, and the average value of the RMPs was -63.10 ± 3.29 mV for controls and -54.33 ± 2.25 mV for AA rats, and a significant difference was observed (control group: $n = 15$ neurons/7 rats; AA group: $n = 19$ neurons/8 rats; one-way ANOVA, $F_{1,32} = 5.13$, $p = 0.030$, Figure 2(b)). We demonstrated RMPs in control and AA rats (Figure 2(c)) and the APs firing pattern of an OXT-mRFP1 neuron in current-clamp mode by induction of currents (from -5 pA to $+5$ pA with $+5$ pA) for 400 ms (Figure 2(d)).

To examine whether the synthesized endogenous OXT affects the RMPs, we recorded the RMPs following the bath application of 1 μM OXT (5 min) to the OXT-mRFP1 neurons in the mPVN of control and AA rats. We show representative RMPs recorded in the OXT-mRFP1 neurons in slices from the control and AA rats (Figure 3(a), top and bottom); 1 μM OXT application increased the RMPs in slices from the control rats (ΔRMPs control group: 3.47 ± 1.80 Hz, $n = 10$ neurons/5 rats), while 1 μM OXT application did not alter the RMPs in slices from the AA rats. The RMPs in the OXT-mRFP1 neurons in the mPVN increased significantly in the AA group compared to that in the control group (ΔRMPs control group: 3.47 ± 1.80 Hz, $n = 10$ neurons/5 rats; group: 0.33 ± 0.71, $n = 8$ neurons/5 rats; one-way ANOVA, $F_{1,16} = -5.10$, $p = 0.00008$, Figure 3(b)).

Next, to examine whether excitatory presynaptic transmitter release changed in the OXT-ergic neurons after chronic inflammation, we recorded sEPSCs and mEPSCs in the OXT-mRFP1 neurons of the mPVN in control and AA rats. We show representative sEPSCs
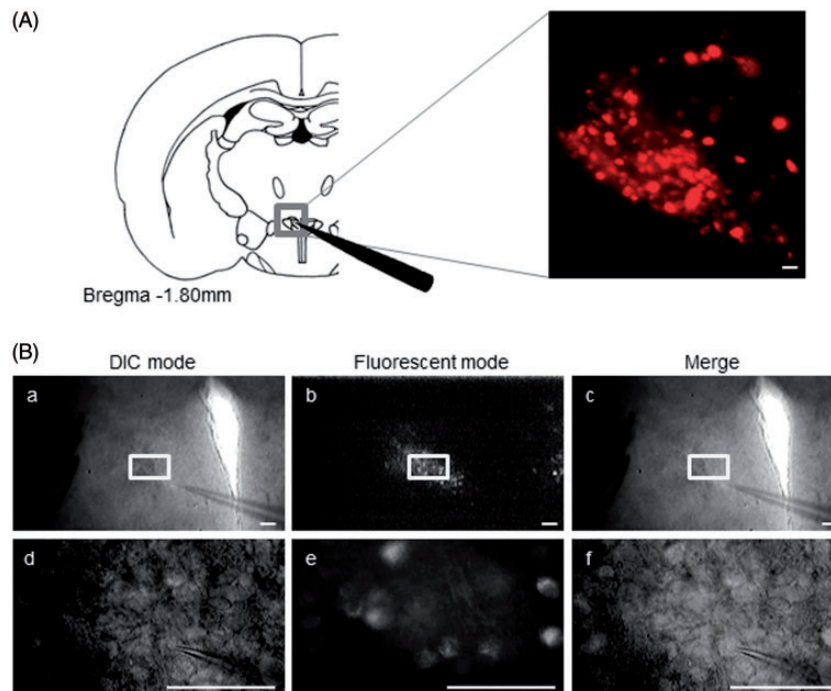
Figure 1. *In vitro* whole-cell patch-clamp recording of neurons in the hypothalamic PVN in the OXT-mRFP1 transgenic rat (A) Left: Schematic drawing of a coronal brain slice including the PVN. Right: OXT-mRFP1 neurons are shown in 300 μm slice including the PVN using fluorescence microscopy. (B) OXT-mRFP1 neurons are distinguished from other neurons by DIC and fluorescence microscopy. DIC mode (B-a and B-d), fluorescent mode (B-b and B-e), and the merged images (B-c and B-f) are shown. B-d to f are shown with high-magnified images of B-a to B-c boxed regions. Scale bars = 100 μm in A right and B.
DIC: differential interference contrast.

and mEPSCs recorded in the OXT-mRFP1 neurons in slices from control and AA rats at a holding potential of −60 mV, and a cumulative histogram of the interevent interval and amplitude (Figure 4(a), (b), (d), and (e)). The frequency of mEPSCs and sEPSCs in OXT-mRFP1 neurons in the mPVN increased significantly in the AA group compared with the control group (sEPSC control group: 1.28 ± 0.16 Hz, $n = 13$ neurons/6 rats; sEPSC AA group: 3.02 ± 0.48, $n = 12$ neurons/6 rats; one-way ANOVA, $F_{1,10} = 12.59$, $p = 0.0017$, Figure 4(c), left) (mEPSC control group: 0.67 ± 0.082 Hz, $n = 34$ neurons/9 rats; mEPSC AA group: 0.88 ± 0.057, $n = 36$ neurons/9 rats; one-way ANOVA, $F_{1,68} = 4.53$, $p = 0.037$, Figure 4(f), left). The amplitude of mEPSCs and sEPSCs in the OXT-mRFP1 neurons in the mPVN was not significantly different between control and AA groups (Figure 4(c) and (f), right).

We investigated whether synthesized OXT from AA rats affects the EPSPs in OXT-ergic neurons. We used a bath application of the OXT receptor antagonist L-368,899.[21] The results show representative sEPSCs and mEPSCs recorded in the OXT-mRFP1 neurons in slices from control and AA rats at a holding potential of −60 mV (Figure 5(a) and (d)). Bath application of L-368,899 dose-dependently increased the frequency of

mEPSCs and sEPSCs in OXT-mRFP1 neurons in AA rats (sEPSC; 10 nM: $111.30 \pm 11.68\%$ of baseline, $t(10) = 0.96$, $p = 0.38$; 100 nM: $145.58 \pm 24.11\%$ of baseline, $t(10) = 1.89$, $p = 0.088$; 1 μM: $154.37 \pm 14.85\%$ of baseline, $t(10) = 3.66$, $p = 0.0043$, paired t test, $n = 6$ neurons/3 rats, Figure 5(b), right) (mEPSC; 10 nM: $102.66 \pm 9.36\%$ of baseline, $t(10) = 0.28$, $p = 0.79$; 100 nM: $169.05 \pm 16.09\%$ of baseline, $t(10) = 4.08$, $p = 0.015$; 1 μM: $235.24 \pm 39.14\%$ of baseline, $t(10) = 3.46$, $p = 0.026$, paired t test, $n = 6$ neurons/3 rats, Figure 5(e), right); however, there was no change in the control rats (sEPSC; 10 nM: $107.99 \pm 9.87\%$ of baseline, $t(10) = 0.81$, $p = 0.45$; 100 nM: $108.23 \pm 8.53\%$ of baseline, $t(10) = 7.74$, $p = 0.96$; 1 μM: $103.39 \pm 6.96\%$ of baseline, $t(10) = 0.48$, $p = 0.64$, paired t test, $n = 6$ neurons/3 rats, Figure 5(b), left) (mEPSC; 10 nM: $99.01 \pm 8.80\%$ of baseline, $t(10) = 0.11$, $p = 0.91$; 100 nM: $105.46 \pm 13.54\%$ of baseline, $t(10) = 0.40$, $p = 0.69$; 1 μM: $101.91 \pm 8.77\%$ of baseline, $t(10) = 0.22$, $p = 0.82$, paired t test, $n = 6$ neurons/3 rats, Figure 5(e), left). Bath application of L-368,899 did not change the amplitude of mEPSCs and sEPSCs in the OXT-mRFP1 neurons in control and AA rats (Figure 5(c) and (f)).

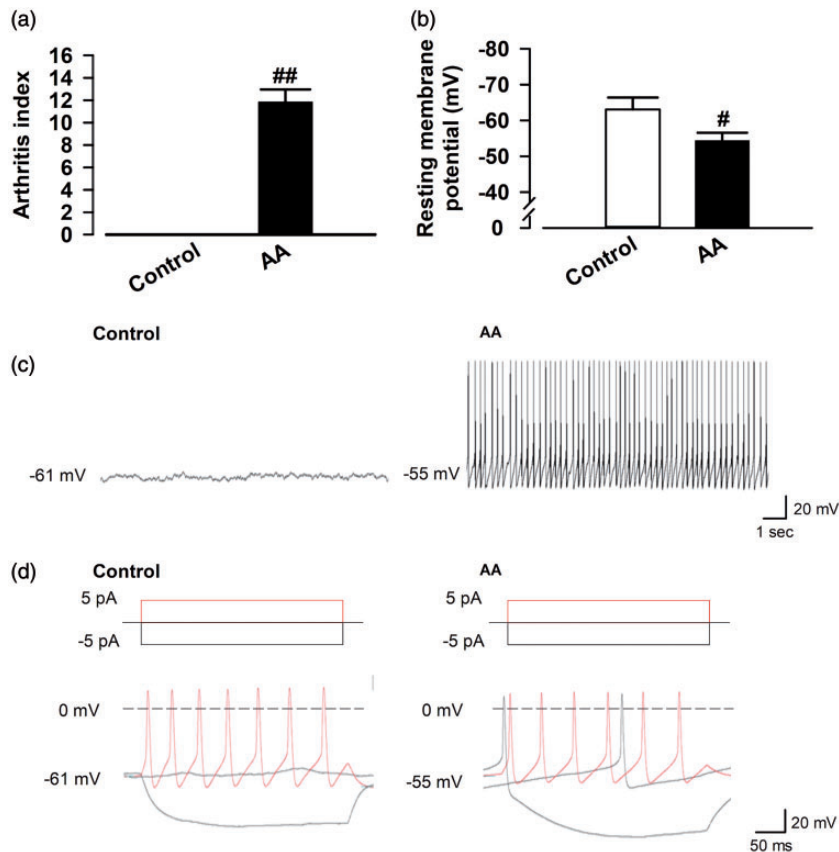We also recorded mIPSCs in OXT-mRFP1 neurons in the mPVN of control and AA rats to examine

Figure 2. Electrophysiological response of OXT-mRFP1 neurons in the magnocellular PVN using whole-cell patch-clamp recordings. (a) The arthritis index in control and AA rats (control group: $n = 6$ rats; AA group: $n = 6$ rats). (b) Representative pooled results showing resting membrane potentials (RMPs) (mV) in control and AA rats (control group: $n = 15$ neurons/7 rats; AA group: $n = 19$ neurons/8 rats). (c) Representative RMPs in control and AA rats. (d) Example AP firing pattern of an OXT-mRFP1 neuron in current-clamp mode by induction of currents in control and AA rat (from -5 pA to $+5$ pA with 5 pA) for 400 ms. $^{\#}p < 0.05$ and $^{\#\#\#}p < 0.01$ compared with control. AA: adjuvant arthritis.

whether inhibitory presynaptic transmitter release changed in the OXT-ergic neurons after chronic inflammation. Representative mIPSCs recorded in the OXT-mRFP1 neurons in slices from control and AA rats at a holding potential of 0 mV, and a cumulative histogram of interevent intervals and amplitudes is shown in Figure 6(a) and (b). The frequency of mIPSCs in OXT-mRFP1 neurons in the mPVN significantly increased in the AA group compared with that in the control group (mIPSC control group: 3.88 ± 0.33 Hz, $n = 21$ neurons/7 rats; mIPSC AA group: 5.50 ± 0.69, $n = 21$ neurons/7 rats; one-way ANOVA, $F_{1,40} = 4.47$, $p = 0.041$, Figure 6(c), left). The amplitude of mIPSCs in OXT-mRFP1 neurons in the mPVN was not significantly different between the control and AA groups (Figure 6(c), right).

In addition, we investigated whether synthesized OXT from AA rats affects the IPSCs in OXT-ergic neurons. The results show representative mIPSCs recorded in the OXT-mRFP1 neurons in slices from control and

AA rats at a holding potential of 0 mV (Figure 6(d)). Bath application of L-368,899 did not change the frequency and amplitude of mIPSCs in OXT-mRFP1 neurons of the control and AA rats (each group: $n = 9$ neurons/5 rats, Figure 6(e) and (f)).

Therefore, the results suggest that feedback of mEPSCs and sEPSCs from synthesized OXT occurs in OXT-ergic neurons in AA rats.

Examination of retrograde transmitters in the feedback system in OXT-mRFP1 neurons in AA rats. Previous studies have demonstrated that regarding feedback in central neurons, retrograde synaptic transmission is known to occur via transmitters such as the nitric oxide (NO), cannabinoid receptor 1 (CB$_1$), and γ-aminobutyric acid (GABA).[22–24] Thus, we investigated whether these transmitters were involved in the feedback from synthesized OXT in AA rats. Following bath application of the GABA$_A$ receptor antagonist (100 μM picrotoxin) (Figure 7(a) and (b)) and CB$_1$ antagonist (2 μM AM 251) (Figure 7(c) and (d)),
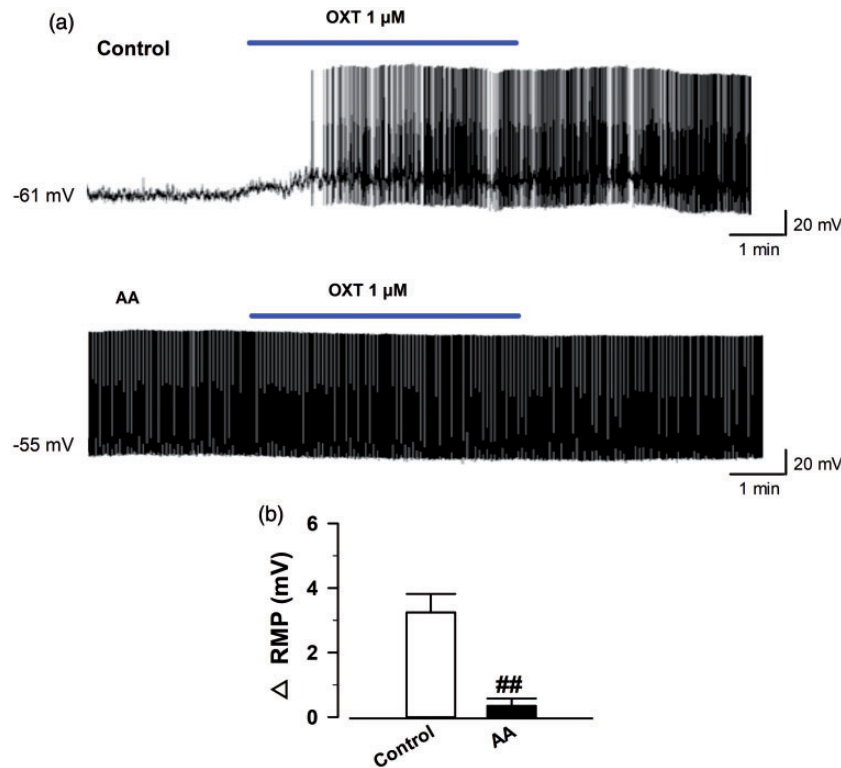
Figure 3. Effect of bath application of OXT on RMPs in OXT-mRFP1 neurons in slices from control and AA rats. (a) Example RMPs traces in the OXT-mRFP1 neurons in slices from control (top) and AA (bottom) rats. (b) Summary RMPs change data of OXT (1 μM) in control and AA rats (control group, $n = 9$ neurons/5 rats, AA group, $n = 8$ neurons/5 rats) $^{\#\#}p < 0.01$ compared with baseline. AA: adjuvant arthritis; RMP: resting membrane potential; OXT: oxytocin.

bath application of L-368,899 still increased the frequency of mEPSCs (picrotoxin; 100 μM picrotoxin: $125.41 \pm 10.7\%$ of baseline, $t(10) = 2.52$, $p = 0.040$, 10 nM L-368,899: $129.25 \pm 7.20\%$ of baseline, $t(10) = 4.06$, $p = 0.0066$; 100 nM L-368,899: $133.87 \pm 6.48\%$ of baseline, $t(10) = 5.23$, $p = 0.0034$; 1 μM L-368,899: $194.97 \pm 20.36\%$ of baseline, $t(10) = 4.66$, $p = 0.00522$, paired t test, $n = 6$ neurons/3 rats, Figure 7(b), left) (AM 251; 2 μM AM 251: $111.53 \pm 8.28\%$ of baseline, $t(10) = 1.39$, $p = 0.23$, 10 nM L-368,899: $117.97 \pm 13.87\%$ of baseline, $t(10) = 1.30$, $p = 0.26$; 100 nM L-368,899: $139.42 \pm 6.00\%$ of baseline, $t(10) = 6.57$, $p = 0.0028$; 1 μM L-368,899: $215.11 \pm 20.70\%$ of baseline, $t(10) = 5.56$, $p = 0.00512$, paired t test, $n = 6$ neurons/3 rats, Figure 7(d), left) and did not change the amplitude of mEPSCs from baseline (Figure 7(b), right and (d), right). However, following the bath application of the NO synthase (NOS) inhibitor (100 μM L-NAME), bath application of L-368,899 did not change the frequency (L-NAME; 100 μM L-NAME: $99.94 \pm 4.39\%$ of baseline, $t(10) = 0.08$, $p = 0.94$, 10 nM L-368,899: $107.30 \pm 5.80\%$ of baseline, $t(10) = 1.26$, $p = 0.26$; 100 nM L-368,899: $101.48 \pm 11.34\%$ of baseline, $t(10) = 0.13$, $p = 0.90$; 1 μM L-

368,899: $106.34 \pm 8.15\%$ of baseline, $t(10) = 0.778$, $p = 0.48$, paired t test, $n = 6$ neurons/3 rats, Figure 7(f), left) or amplitude of mEPSCs in the AA rats (Figure 7(f), right). Furthermore, mEPSCs increased significantly from baseline only following the bath application of picrotoxin (paired t test, $p < 0.05$). Therefore, this suggests that NOS contributes to the feedback system of synthesized OXT in AA rats.

Confirmation of the effect of OXT and the OXT receptor antagonist L-368,899 in OXT-mRFP1 neurons in slices from control and AA rats. We confirmed the effects of OXT and L-368,899 in the OXT-mRFP1 neurons. After recording a stable baseline at a holding potential of -60 mV, we recorded mEPSCs following the application of 1 μM OXT and different doses of L368,899 (10 and 100 nM and 1 μM) on mEPSCs in the OXT-mRFP1 neurons in control rats and the application of 1 μM OXT on mEPSCs in the OXT-mRFP1 neurons in AA rats. Following the bath application of OXT, the frequency of mEPSCs in OXT-mRFP1 neurons was significantly increased (OXT; 1 μM OXT: $233.45 \pm 25.99\%$ of baseline, $t(10) = 5.1$, $p = 0.00215$, $n = 6$ neurons/4 rats, Figure 8(b), left) in the control rats, while OXT did not change the amplitude of mEPSCs (Figure 8(b), right).
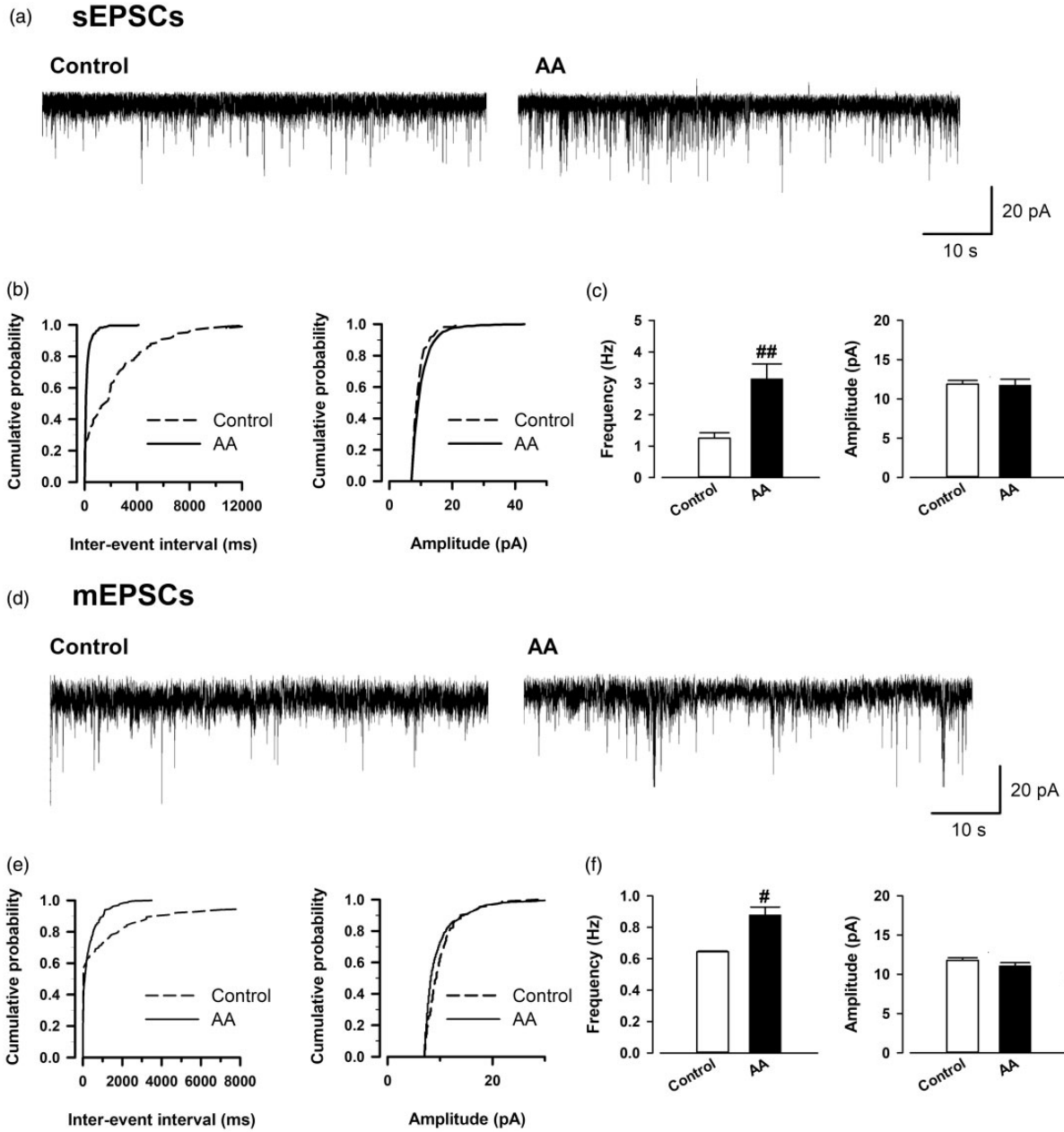
(a) **sEPSCs**

Control   **AA**

(b)

(c)

(d) **mEPSCs**

Control   **AA**

(e)

(f)

Figure 4. sEPSCs and mEPSCs recorded in the OXT-mRFP1 neurons in control and AA rats. (a, d) Representative sEPSCs and mEPSCs recorded in the OXT-mRFP1 neuron in slices from a control rat (left) and AA rat (right) at a holding potential of -60 mV. Cumulative interevent interval (left) and amplitude (right) histograms of sEPSCs (b) and mEPSCs (e) recorded in slices from control rats (sEPSCs; $n = 13$ neurons/6 rats, mEPSCs; $n = 34$ neurons/9 rats) and AA rats (sEPSCs; $n = 12$ neurons/6 rats, mEPSCs; $n = 36$ neurons/9 rats). (c and f) Summary frequency (left) and amplitude (right) of sEPSC and mEPSCs data. $^{\#}p < 0.05$ and $^{\#\#}p < 0.01$ compared with control. AA: adjuvant arthritis; mEPSC: miniature excitatory postsynaptic current; sEPSC: spontaneous excitatory postsynaptic current.

After application of L-368,899, the increased frequency of mEPSCs returned to baseline in a dose-dependent manner (10 nM L-368,899: $210.16 \pm 18.37\%$ of baseline, $t(10) = 5.99$, $p = 0.00185$; 100 nM L-368,899: $125.75 \pm 18.81\%$ of baseline, $t(10) = 1.37$, $p = 0.22$; 1 μM L-368,899: $98.66 \pm 10.17\%$ of baseline, $t(10) = 0.13$, $p = 0.90$, paired t test, $n = 6$ neurons/3 rats, Figure 8(b), left), but the amplitude of mEPSCs remained unchanged (Figure 8(b), right). In AA rats, the bath application of OXT did not change both the frequency (OXT; 1 μM OXT: $92.52 \pm 14.79\%$ of baseline, $t(8) = 1.43$, $p = 0.195$, $n = 8$ neurons/5 rats, Figure 8(d), left) and the amplitude (OXT; 1 μM OXT: $98.41 \pm 6.81\%$ of baseline, $t(8) = 1.16$, $p = 0.274$, $n = 8$ neurons/5 rats, Figure 8(d), right) of mEPSCs (Figure, 8(d)).
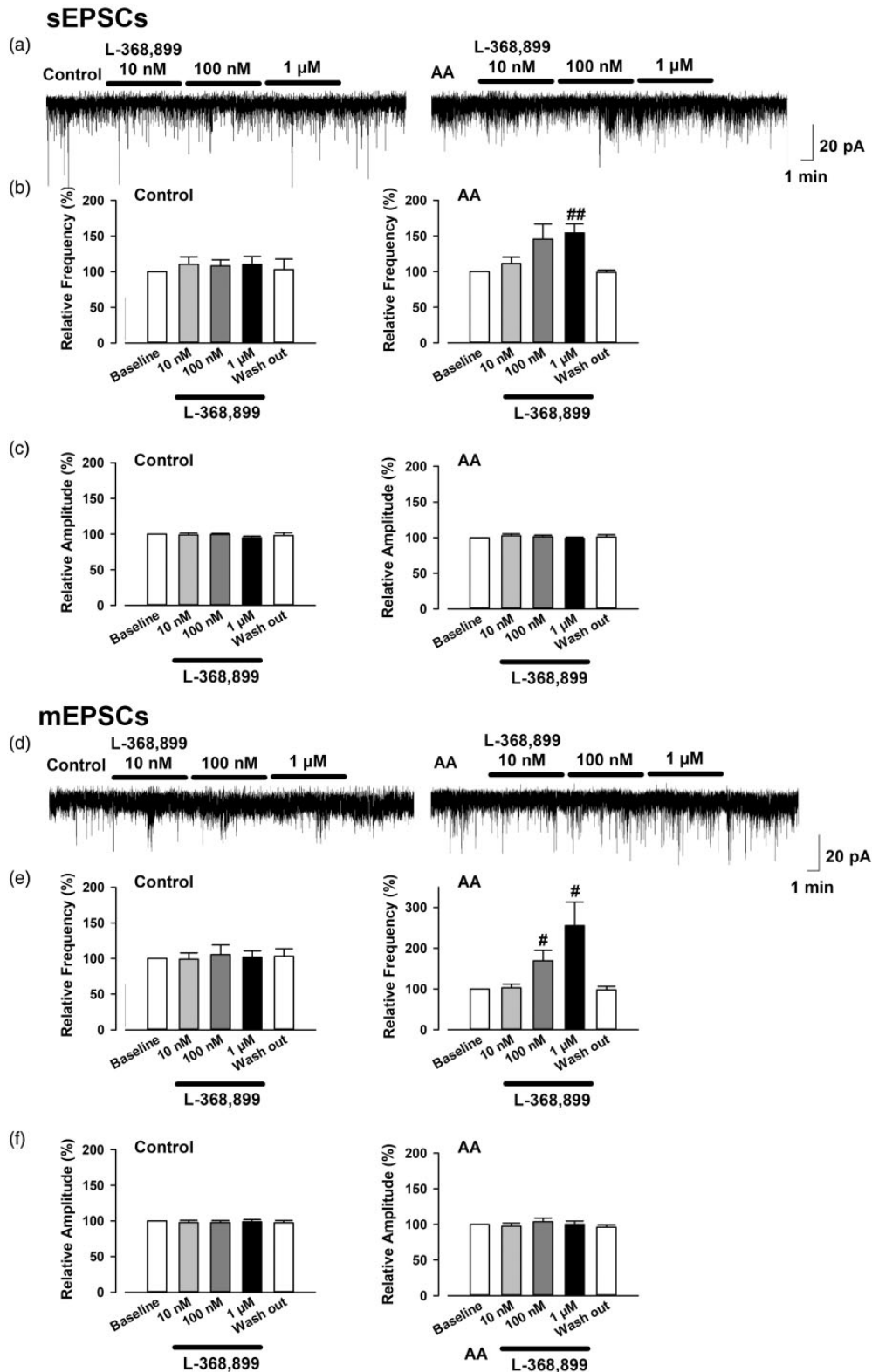
Figure 5. Effect of bath application of L368,899 on sEPSCs and mEPSCs in OXT-mRFP1 neurons in slices from control (left) and AA (right) rats. Example sEPSC (a) and mEPSC (d) traces are shown. Summary frequency data of the different doses of L368,899 (10 and 100 nM and 1 μM) on sEPSCs (b) and mEPSCs (e). Summary amplitude data of the different doses of L368,899 (10 and 100 nM and 1 μM) on sEPSCs (c) and mEPSCs (f) (each group, $n = 6$ neurons/3 rats) $^{#}p < 0.05$ and $^{###}p < 0.01$ compared with baseline.
AA: adjuvant arthritis; mEPSC: miniature excitatory postsynaptic current; sEPSC: spontaneous excitatory postsynaptic current.
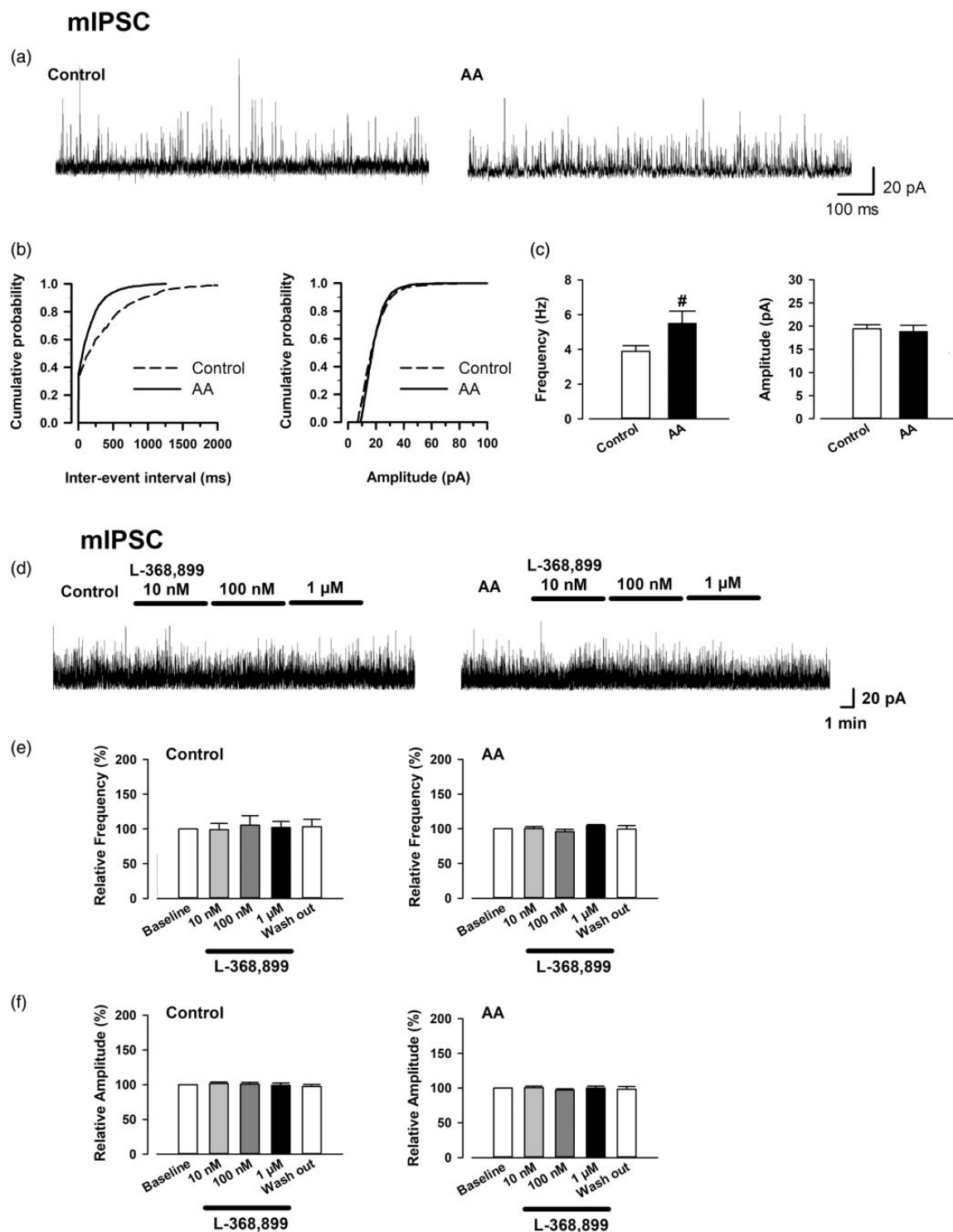
mIPSC

(a)

(b)

(c)

mIPSC

(d)

(e)

(f)

Figure 6. mIPSCs recorded in the OXT-mRFP1 neurons in control and AA rats, and effect of bath application of L368,899 on mIPSCs in OXT-mRFP1 neurons in slices from control (left) and AA (right) rats. (a) Representative mIPSCs recorded in the OXT-mRFP1 neurons in slices from a control rat (left) and AA rat (right) at a holding potential of 0 mV. (b) Cumulative interevent interval (left) and amplitude (right) histograms of mIPSCs recorded in slices from control rats (mIPSCs; $n = 21$ neurons/7 rats) and AA rats (mIPSCs; $n = 20$ neurons/7 rats). (c) Summary frequency (left) and amplitude (right) of mIPSCs data. $^{\#}p < 0.05$ compared with control. (d) Example mIPSC traces are shown. (e) Summary frequency data of the different doses of L368,899 (10 and 100 nM and 1 μM) on mIPSCs. (f) Summary amplitude data of the different doses of L368,899 (10 and 100 nM and 1 μM) on mIPSCs (each group, $n = 9$ neurons/5 rats).
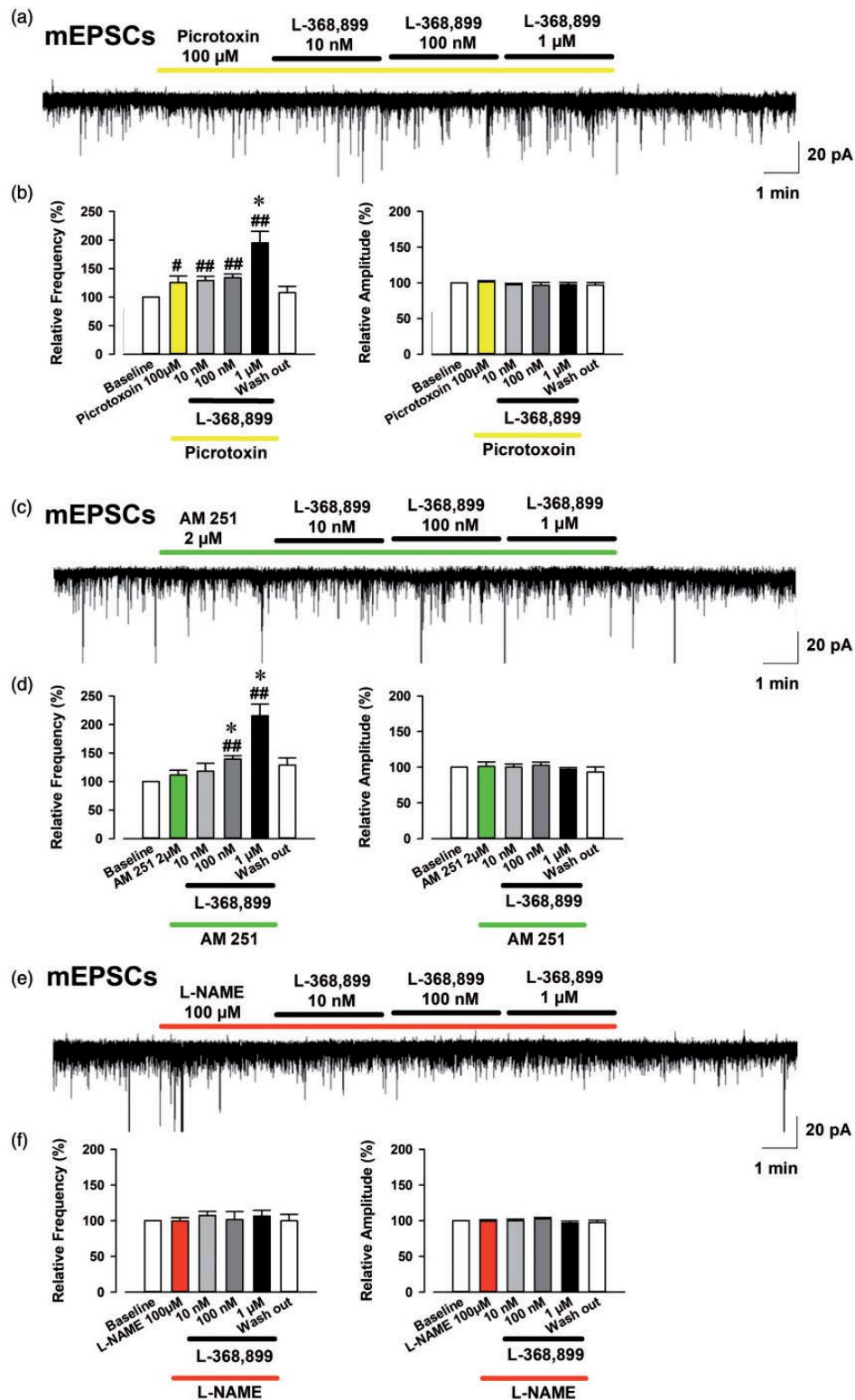AA: adjuvant arthritis; mIPSC: miniature inhibitory postsynaptic current.

Figure 7. Effect of bath application of picrotoxin, AM 251, and L-NAME on induced mEPSCs increased by L-368,899 in OXT-mRFP1 neurons in slices from AA rats. Example trace of mEPSCs following the bath application of 100 μM picrotoxin (a), 2 μM AM 251 (c), and 100 μM L-NAME (e) after the bath application of L-368,899 in OXT-mRFP1 neurons in AA rats are shown. Summary frequency (left) and amplitude (right) data of the effect of picrotoxin (b), AM 251 (d), and L-NAME (f) after the bath application of L-368,899 in OXT-mRFP1 neurons in AA rats (each group, $n = 6$ neurons/3 rats). [#]$p < 0.05$ and [##]$p < 0.01$ compared with baseline. [*]$p < 0.05$ compared with only 100 μM picrotoxin or 2 μM AM 251.

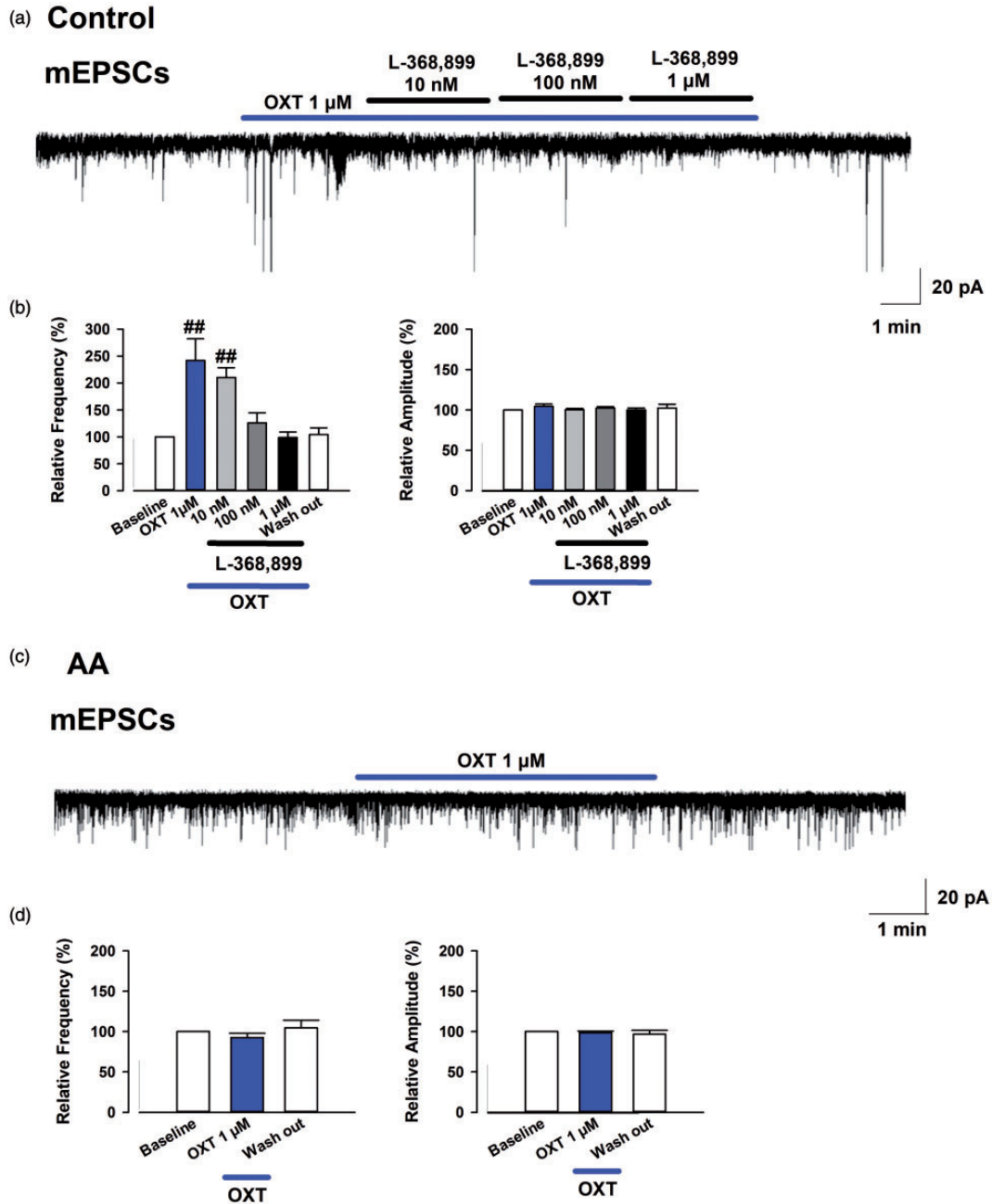mEPSC: miniature excitatory postsynaptic current.

Figure 8. Effect of bath application of OXT and L-368,899 on mEPSCs in OXT-mRFP1 neurons in slices from control and AA rats. (a) Example trace of mEPSCs following the application of 1 μM OXT and different doses of L368,899 (10 and 100 nM and 1 μM) on mEPSCs in OXT-mRFP1 neurons in control rats are shown. (b) Summary frequency (left) and amplitude (right) data of 1 μM OXT and different doses of L368,899 (10 and 100 nM and 1 μM) on mEPSCs in OXT-mRFP1 neurons in control rats (each drug group, $n = 6$ neurons/4 rats). (c) Example trace of mEPSCs following the application of 1 μM OXT on mEPSCs in the OXT-mRFP1 neurons in AA rats. (d) Summary frequency (left) and amplitude (right) data of 1 μM OXT on mEPSCs in the OXT-mRFP1 neurons in the AA rats (each drug group, $n = 8$ neurons/5 rats). [##]$p < 0.01$ compared with baseline.
AA: adjuvant arthritis; OXT: oxytocin; mEPSC: miniature excitatory postsynaptic current.

We confirmed that the bath application OXT affects the presynaptic current in OXT-mRFP1 neurons in the control rats, and L-368,899 inhibited the effect of OXT. However, the bath application OXT did not affect the presynaptic current in OXT-mRFP1 neurons in the AA rats.

A hypothetical scheme for the excitatory system, the inhibitory system, and the feedback mechanism of OXT-
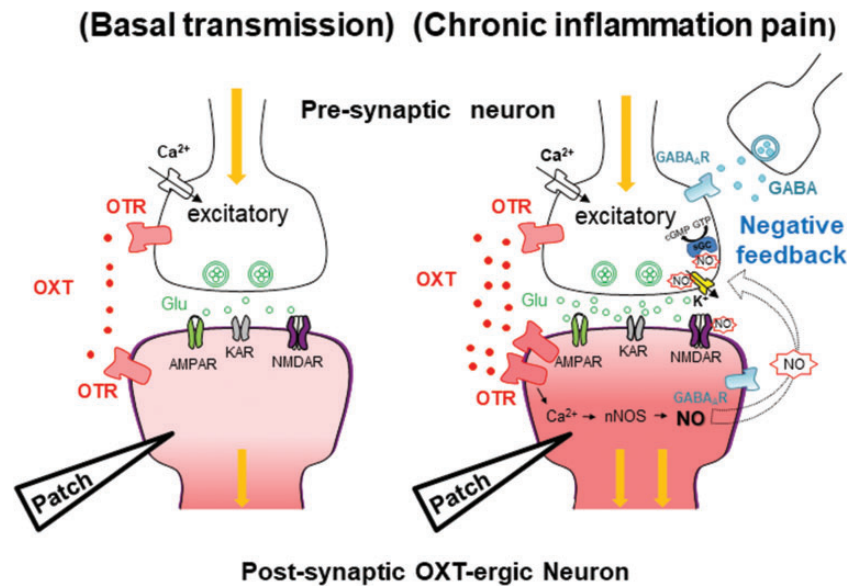
(Basal transmission) (Chronic inflammation pain)

Figure 9. A hypothetical scheme for the excitatory system, the inhibitory system, and the feedback mechanism of OXT-ergic neurons in the hypothalamus in the rat chronic inflammation model. (Left) Basal transmission: OTR is present in both excitatory pre- and postsynaptic neurons in OXT-ergic neurons. (Right) Chronic inflammation pain: Chronic inflammation pain enhances synaptic excitatory and inhibitory transmissions. Activated OXT works as negative feedback excitatory system around itself via the OTR. The signaling pathway of the negative feedback system contributes to the nNOS to promote NO production. NO and GABA act as retrograde neurotransmitters causing negative feedback at the pre-or postsynaptic OXT-ergic neurons.
GABA: γ-aminobutyric acid ; AMPAR: α-amino-3-hydroxy-5-methyl-4-isoxazolepropionic acid receptor ; KAR: Kainate type glutamate receptor ; NMDAR: N-methyl-D-aspartic acid receptor ; OXT: oxytocin; OTR: OXT receptor; nNOS: neuronal nitric oxide synthase; NO: nitric oxide.

ergic neurons in the hypothalamus of the chronic inflammation rat model is shown in Figure 9.

Discussion

In this study, we investigated RMPs, mEPSCs, and sEPSCs in the OXT-ergic neurons of the mPVN by using OXT-mRFP1 transgenic rats with AA. We have demonstrated that the RMPs and the frequency of mEPSCs and sEPSCs in the absence of picrotoxin, or mIPSCs were increased in OXT-mRFP1 neurons in the mPVN of AA rats. Furthermore, the feedback system of synthesized endogenous OXT was also investigated using L-368,899. L-368,899 dose-dependently further increased the frequency of mEPSCs and sEPSCs in the neurons of AA rats. Following the bath application of picrotoxin and AM 251, L-368,899 still increased the frequency of mEPSCs in the AA rats. However, following the bath application of L-NAME, L-368,899 did not change the frequency of mEPSCs in AA rats. Our results indicate that the activity of OXT-ergic neurons is upregulated by increasing the glutamate release in AA rats, and upregulated OXT neurons have a feedback system with the released OXT. It is possible that NO and not GABA may contribute to the feedback system in OXT neurons in AA rats.

A previous study demonstrated that *OXT* and *mRFP1* mRNA and the red fluorescence intensity of mRFP1 were increased in the PVN of rats at 15 and 22 days after the onset of arthritis in OXT-mRFP1 transgenic rats. OXT-mRFP1 fluorescence intensity has also been shown to be increased in the dorsal horn of the spinal cord and posterior pituitary in AA rats.[12] These results suggest that OXT was upregulated in both the hypothalamo-neurohypophysial and hypothalamo-spinal pathways by chronic inflammation.

In this study, we focused on the increase of the release probability for the glutamate and surrounding synthesized OXT. Glutamate is the main excitatory neurotransmitter, and the glutamate receptor is critical for synaptic plasticity. In animals of chronic pain model, the glutamate is increased in various neurons such as the substantia gelatinosa neuron of the spinal cord dorsal horn and the pyramidal neuron of the anterior cingulate cortex, which play an important role in the pain perception.[25–27] The increased glutamate induces a long-term potentiation, which is proposed to be the cellular model for learning and memory.[28] OXT also enhances the synaptic transmission in the hippocampus *in vitro*.[29,30] We hypothesize that the upregulated OXT-ergic mechanism is associated with the presynaptic glutamate release and the surrounding synthesized OXT,

which work as neurotransmitters in the upregulated OXT-ergic neuron. We show that the enhancement in the synaptic transmission is the result of an increased presynaptic probability of the neurotransmitter release in the hypothalamus synapses, as demonstrated by the increased mEPSC frequency in the chronic inflammation model. The hypothalamic OXT-ergic neurons likely have also already undergone plasticity changes by the synthesized endogenous OXT as the bath application of OXT did not change the frequency of mEPSCs in the AA rats.

Interestingly, AA rats produced an increase of RMPs compared to the control rats. Furthermore, the bath application of OXT produced an increase of RMPs in the OXT-mRFP1 neurons of the control rats; however, the bath application of OXT did not change the RMPs in the AA rats. The results demonstrate that surrounding synthesized endogenous OXT may have already produced an increase of the RMPs in the OXT-ergic neurons in the AA rats. Increased APs have been reported in the spinal cord dorsal horn in rats of a chronic pain model without any change in the RMPs.[25] In the hypothalamic OXT-ergic neuron, a chronic inflammation model such as the AA rats induces the increase of APs; RMPs are also increased by the surrounding synthesized endogenous OXT. Although the mechanisms to produce APs and increase of RMPs are not yet fully understood, endogenous OXT may depolarize the OXT-ergic neurons, and this depolarization may be mediated by L-type Ca channel.[31] Taken together, these results suggest that the presynaptic glutamate release and the synthesized endogenous OXT are the factors that upregulate activity in the OXT-ergic neurons.

We also found that L-368,899 dose-dependently increased the frequency of mEPSCs and sEPSCs in OXT-mRFP1 neurons in AA rats, suggesting that the activity of presynaptic excitatory neurons was suppressed by increasing OXT in the AA model. In this study, it is unclear which OXT-ergic neurons secrete OXT. It is possible that one of the major pathways involved in the secretion of OXT is the paracrine,[32] which is thought to enter the ventricle and act on the OXT receptor after release from the PVN.[33] OXT is also synthesized in the parvocellular PVN neurons, and some of these neurons are thought to project to the magnocellular PVN OXT neurons.[3] Consequently, it is assumed that the synthesized endogenous OXT suppressed the excitatory neurotransmission in the surrounding or its own OXT neurons in AA rats as a feedback system. In previous studies, it was unclear how feedback was provided to OXT neurons in the central nervous system. At the spinal level, OXT activates the presynaptic OXT receptor at the glutamatergic interneuron ends and promotes the synaptic release of glutamate and inhibitory GABA-ergic interneurons.[34] Therefore, OXT may activate the excitatory and inhibitory neurons by stimulating the presynaptic OXT receptor in the central nervous system.

Meanwhile, there is a mechanism that uses a retrograde transmitter as a mechanism for feedback through the postsynaptic OXT receptor. NO has been shown to be present in the central nervous system[35] and has long been considered a retrograde neurotransmitter because it is a fat-soluble gas that diffuses across cell membranes.[36] Neuronal NOS (nNOS) is abundant in the PVN, and nNOS in the PVN has been shown to be increased in several rat models of stress.[37–39] It has been suggested that NO plays a role as an important messenger in the PVN-spinal pathway and may act in concert with OXT.[40]

NO synthesis is competitively inhibited by L-NAME, which has a similar structure to the L-arginine.[41] L-NAME suppresses the hippocampal long-term potentiation, and it has been reported that NO may be a hippocampal retrograde transmitter.[42] On the other hand, it has been suggested that NO is also associated with signaling via the OXT receptor. Exogenous OXT hyperpolarizes the dorsal root ganglia neurons that induce the feeling of pain in rats, and that this hyperpolarization is mediated by the Ca^{2+}/nNOS/NO/K_{ATP} pathway.[43] NO is also associated with other neuronal signal pathways, such as the NO/sGC/cGMP pathway, and downregulation of N-methyl-D-aspartic acid (NMDA)-receptor activity by reaction with thiol group (s) of the NMDA receptor's redox modulatory site.[44,45] Thus, released OXT may cause hyperpolarization and downregulation of NMDA-receptor activity in several putative pathways in the AA rats. As a result, OXT may modulate the glutamine release though the OXT receptor in OXT-mRFP1 neurons. Pretreatment with the OXT receptor antagonist Atociban or the selective NOS inhibitor N-propyl-L-arginine significantly attenuates the hyperpolarization caused by OXT.[43]

We found that OXT-ergic neurons generate negative feedback with OXT itself in the PVN in AA rats. In addition, NO is a contributor to the feedback mechanism.

Although we investigated the contribution of $GABA_A$ to the feedback system through the OXT receptors, increased mEPSCs induced by the OXT receptor antagonist did not change following the bath application of the $GABA_A$ antagonist. It is thought that $GABA_A$ is not related to the feedback system through OXT receptors. Instead, $GABA_A$ may work as a retrograde transmitter in other feedback systems that are not related to the OXT receptor.

A limitation of the study is that the evoked EPSC was not investigated. Thus, we did not examine the postsynaptic changes of the OXT-ergic neurons in AA rats. Moreover, the relationship between OXT-ergic neurons

was not described. In the future, the plasticity of OXT-mRFP1 neurons should be examined, and paired recordings with OXT-mRFP1 neurons should be conducted.

In conclusion, the activity of OXT-ergic neurons is upregulated by increasing the glutamate release in AA rats, and OXT neurons have a feedback system with released OXT. It is possible that NOS may contribute to the feedback system of the OXT-ergic neurons.

Author Contributions

TM designed the project. TF and TM performed the electrophysiological experiments. TF, TM, and MK wrote the initial draft and finished the final version of the manuscript. HS, HN, KB, YY, HO, YU, and AS contributed to the analysis and interpretation of data and assisted in the preparation of the manuscript. All authors read and approved the final manuscript.

Declaration of Conflicting Interests

The author(s) declared no potential conflicts of interest with respect to the research, authorship, and/or publication of this article.

ORCID iD

Makoto Kawasaki https://orcid.org/0000-0001-8410-5800

References

1. Higashida H, Lopatina O, Yoshihara T, Pichugina YA, Soumarokov AA, Munesue T, Minabe Y, Kikuchi M, Ono Y, Korshunova N, Salmina AB. Oxytocin signal and social behaviour: comparison among adult and infant oxytocin, oxytocin receptor and CD38 gene knockout mice. *J Neuroendocrinol* 2010; 22: 373–379.
2. Pedersen CA, Vadlamudi SV, Boccia ML, Amico JA. Maternal behavior deficits in nulliparous oxytocin knockout mice. *Genes Brain Behav* 2006; 5: 274–281.
3. Eliava M, Melchior M, Knobloch-Bollmann HS, Wahis J, da Silva Gouveia M, Tang Y, Ciobanu AC, Triana Del Rio R, Roth LC, Althammer F, Chavant V, Goumon Y, Gruber T, Petit-Demoulière N, Busnelli M, Chini B, Tan LL, Mitre M, Froemke RC, Chao MV, Giese G, Sprengel R, Kuner R, Poisbeau P, Seeburg PH, Stoop R, Charlet A, Grinevich V. A new population of parvocellular oxytocin

neurons controlling magnocellular neuron activity and inflammatory pain processing. *Neuron* 2016; 89: 1291–1304.
4. Petersson M, Wiberg U, Lundeberg T, Uvnäs-Moberg K. Oxytocin decreases carrageenan induced inflammation in rats. *Peptides* 2001; 22: 1479–1484.
5. DeLaTorre S, Rojas-Piloni G, Martínez-Lorenzana G, Rodríguez-Jiménez J, Villanueva L, Condés-Lara M. Paraventricular oxytocinergic hypothalamic prevention or interruption of long-term potentiation in dorsal horn nociceptive neurons: electrophysiological and behavioral evidence. *Pain* 2009; 144: 320–328.
6. Gutierrez S, Liu B, Hayashida K, Houle TT, Eisenach JC. Reversal of peripheral nerve injury-induced hypersensitivity in the postpartum period: role of spinal oxytocin. *Anesthesiology* 2013; 118: 152–116.
7. Onaka T, Palmer JR, Yagi K. A selective role of brainstem noradrenergic neurons in oxytocin release from the neurohypophysis following noxious stimuli in the rat. *Neurosci Res* 1996; 25: 67–75.
8. Onaka T. Catecholaminergic mechanisms underlying neurohypophysial hormone responses to unconditioned or conditioned aversive stimuli in rats. *Exp Physiol* 2000; 85: 101s–110s.
9. Onaka T. Neural pathways controlling central and peripheral oxytocin release during stress. *J Neuroendocrinol* 2004; 16: 308–312.
10. Matsuura T, Kawasaki M, Hashimoto H, Yoshimura M, Motojima Y, Saito R, Ueno H, Maruyama T, Ishikura T, Sabanai K, Mori T, Ohnishi H, Onaka T, Sakai A, Ueta Y. Possible involvement of the rat hypothalamo-neurohypophysial/-spinal oxytocinergic pathways in acute nociceptive responses. *J Neuroendocrinol* 2016; 28: 10.1111/jne.12396.
11. Russell J, Leng G, Bicknell R. Opioid tolerance and dependence in the magnocellular oxytocin system: a physiological mechanism? *Exp Physiol* 1995; 80: 307–340.
12. Matsuura T, Kawasaki M, Hashimoto H, Ishikura T, Yoshimura M, Ohkubo JI, Maruyama T, Motojima Y, Sabanai K, Mori T, Ohnishi H, Sakai A, Ueta Y. Fluorescent visualisation of oxytocin in the hypothalamo-neurohypophysial/-spinal pathways after chronic inflammation in oxytocin-monomeric red fluorescent protein 1 transgenic rats. *J Neuroendocrinol* 2015; 27: 636–646.
13. Koga K, Shimoyama S, Yamada A, Furukawa T, Nikaido Y, Furue H, Nakamura K, Ueno S. Chronic inflammatory pain induced GABAergic synaptic plasticity in the adult mouse anterior cingulate cortex. *Mol Pain* 2018; 14: 1744806918783478–1744806918783414.
14. Son SJ, Filosa JA, Potapenko ES, Biancardi VC, Zheng H, Patel KP, Tobin VA, Ludwig M, Stern JE. Dendritic peptide release mediates interpopulation crosstalk between neurosecretory and preautonomic networks. *Neuron* 2013; 78: 1036–1049.
15. Stern JE. Neuroendocrine-autonomic integration in the paraventricular nucleus: novel roles for dendritically released neuropeptides. *J Neuroendocrinol* 2015; 27: 487–497.

16. Bealer SL, Armstrong WE, Crowley WR. Oxytocin release in magnocellular nuclei: neurochemical mediators and functional significance during gestation. *Am J Physiol Regul Integr Comp Physiol* 2010; 299: R452–R458.

17. Yamashita M, Glasgow E, Zhang BJ, Kusano K, Gainer H. Identification of cell-specific messenger ribonucleic acids in oxytocinergic and vasopressinergic magnocellular neurons in rat supraoptic nucleus by single-cell differential hybridization. *Endocrinology* 2002; 143: 4464–4476.

18. Katoh A, Fujihara H, Ohbuchi T, Onaka T, Hashimoto T, Kawata M, Suzuki H, Ueta Y. Highly visible expression of an oxytocin-monomeric red fluorescent protein 1 fusion gene in the hypothalamus and posterior pituitary of transgenic rats. *Endocrinology* 2011; 152: 2768–2774.

19. Nagatomo T, Inenaga K, Yamashita H. Transient outward current in adult rat supraoptic neurones with slice patch-clamp technique: inhibition by angiotensin II. *J Physiol* 1995; 485: 87–96.

20. Matsuura T, Li XH, Tao C, Zhuo M. Effects of matrix metalloproteinase inhibitors on N-methyl-D-aspartate receptor and contribute to long-term potentiation in the anterior cingulate cortex of adult mice. *Mol Pain* 2019; 15: 1744806919842958–1744806919842910.

21. Evans BE, Leighton JL, Rittle KE, Gilbert KF, Lundell GF, Gould NP, Hobbs DW, DiPardo RM, Veber DF, Pettibone DJ, Clineschmidt BV, Anderson PS, Freidinger RM. Orally active, nonpeptide oxytocin antagonists. *J Med Chem* 1992; 35: 3919–3927.

22. Di S, Maxson MM, Franco A, Tasker JG. Glucocorticoids regulate glutamate and GABA synapse-specific retrograde transmission via divergent nongenomic signaling pathways. *J Neurosci* 2009; 29: 393–401.

23. Ohno-Shosaku T, Maejima T, Kano M. Endogenous cannabinoids mediate retrograde signals from depolarized postsynaptic neurons to presynaptic terminals. *Neuron* 2001; 29: 729–738.

24. Zilberter Y, Harkany T, Holmgren CD. Dendritic release of retrograde messengers controls synaptic transmission in local neocortical networks. *Neuroscientist* 2005; 11: 334–344.

25. Uta D, Kato G, Doi A, Andoh T, Kume T, Yoshimura M, Koga K. Animal models of chronic pain increase spontaneous glutamatergic transmission in adult rat spinal dorsal horn in vitro and in vivo. *Biochem Biophys Res Commun* 2019; 512: 352–359.

26. Zhao M-G, Ko S W, Wu L-J, Toyoda H, Xu H, Quan J, Li J, Jia Y, Ren M, Xu Z C, Zhuo M. Enhanced presynaptic neurotransmitter release in the anterior cingulate cortex of mice with chronic pain. *J Neurosci* 2006; 26: 8923–8930.

27. Bliss TVP, Collingridge GL, Kaang BK, Zhuo M. Synaptic plasticity in the anterior cingulate cortex in acute and chronic pain. *Nat Rev Neurosci* 2016; 17: 485–496.

28. Richter-Levin G, Canevari L, Bliss T. Long-term potentiation and glutamate release in the dentate gyrus: links to spatial learning. *Behav Brain Res* 1995; 66: 37–40.

29. Owen SF, Tuncdemir SN, Bader PL, Tirko NN, Fishell G, Tsien RW. Oxytocin enhances hippocampal spike transmission by modulating fast-spiking interneurons. *Nature* 2013; 500: 458–462.

30. Tomizawa K, Iga N, Lu YF, Moriwaki A, Matsushita M, Li ST, Miyamoto O, Itano T, Matsui H. Oxytocin improves long-lasting spatial memory during motherhood through MAP kinase cascade. *Nat Neurosci* 2003; 6: 384–390.

31. Arrowsmith S, Wray S. Oxytocin: its mechanism of action and receptor signalling in the myometrium. *J Neuroendocrinol* 2014; 26: 356–369.

32. Ludwig M, Pittman QJ. Talking back: dendritic neurotransmitter release. *Trends Neurosci* 2003; 26: 255–261.

33. Striepens N, Kendrick KM, Maier W, Hurlemann R. Prosocial effects of oxytocin and clinical evidence for its therapeutic potential. *Front Neuroendocrinol* 2011; 32: 426–450.

34. Breton JD, Veinante P, Uhl-Bronner S, Vergnano AM, Freund-Mercier MJ, Schlichter R, Poisbeau P. Oxytocin-induced antinociception in the spinal cord is mediated by a subpopulation of glutamatergic neurons in lamina I-II which amplify GABAergic inhibition. *Mol Pain* 2008; 4: 19–12.

35. Garthwaite J, Charles SL, Chess-Williams R. Endothelium-derived relaxing factor release on activation of NMDA receptors suggests role as intercellular messenger in the brain. *Nature* 1988; 336: 385–388.

36. Kerwin JF, Lancaster JR, Feldman PL. Nitric oxide: a new paradigm for second messengers. *J Med Chem* 1995; 38: 4343–4362.

37. Bredt DS, Hwang PM, Snyder SH. Localization of nitric oxide synthase indicating a neural role for nitric oxide. *Nature* 1990; 347: 768–770.

38. Calzà L, Giardino L, Ceccatelli S. NOS mRNA in the paraventricular nucleus of young and old rats after immobilization stress. *Neuroreport* 1993; 4: 627–630.

39. Sánchez F, Moreno MN, Vacas P, Carretero J, Vázquez R. Swim stress enhances the NADPH-diaphorase histochemical staining in the paraventricular nucleus of the hypothalamus. *Brain Res* 1999; 828: 159–162.

40. Nylén A, Skagerberg G, Alm P, Larsson B, Holmqvist B, Andersson KE. Nitric oxide synthase in the hypothalamic paraventricular nucleus of the female rat; organization of spinal projections and coexistence with oxytocin or vasopressin. *Brain Res* 2001; 908: 10–24.

41. Rees DD, Palmer RMJ, Schulz R, Hodson HF, Moncada S. Characterization of three inhibitors of endothelial nitric oxide synthase in vitro and in vivo. *Br J Pharmacol* 1990; 101: 746–752.

42. Schuman EM, Madison DV. A requirement for the intercellular messenger nitric oxide in long-term potentiation. *Science* 1991; 254: 1503–1506.

43. Gong L, Gao F, Li J, Li J, Yu X, Ma X, Zheng W, Cui S, Liu K, Zhang M, Kunze W, Liu CY. Oxytocin-induced membrane hyperpolarization in pain-sensitive dorsal root ganglia neurons mediated by Ca $2+$/nNOS/NO/K ATP pathway. *Neuroscience* 2015; 289: 417–428.

44. Klein C. Nitric oxide and the other cyclic nucleotide. *Cell Signal* 2002; 14: 493–498.

45. Lipton SA, Choi YB, Pan ZH, Lei SZ, Chen HSV, Sucher NJ, Loscalzo J, Singel DJ, Stamler JS. A redox-based mechanism for the neuroprotective and neurodestructive effects of nitric oxide and related nitroso-compounds. *Nature* 1993; 364: 626–632.